DOI: 10.1002/chem.200601560

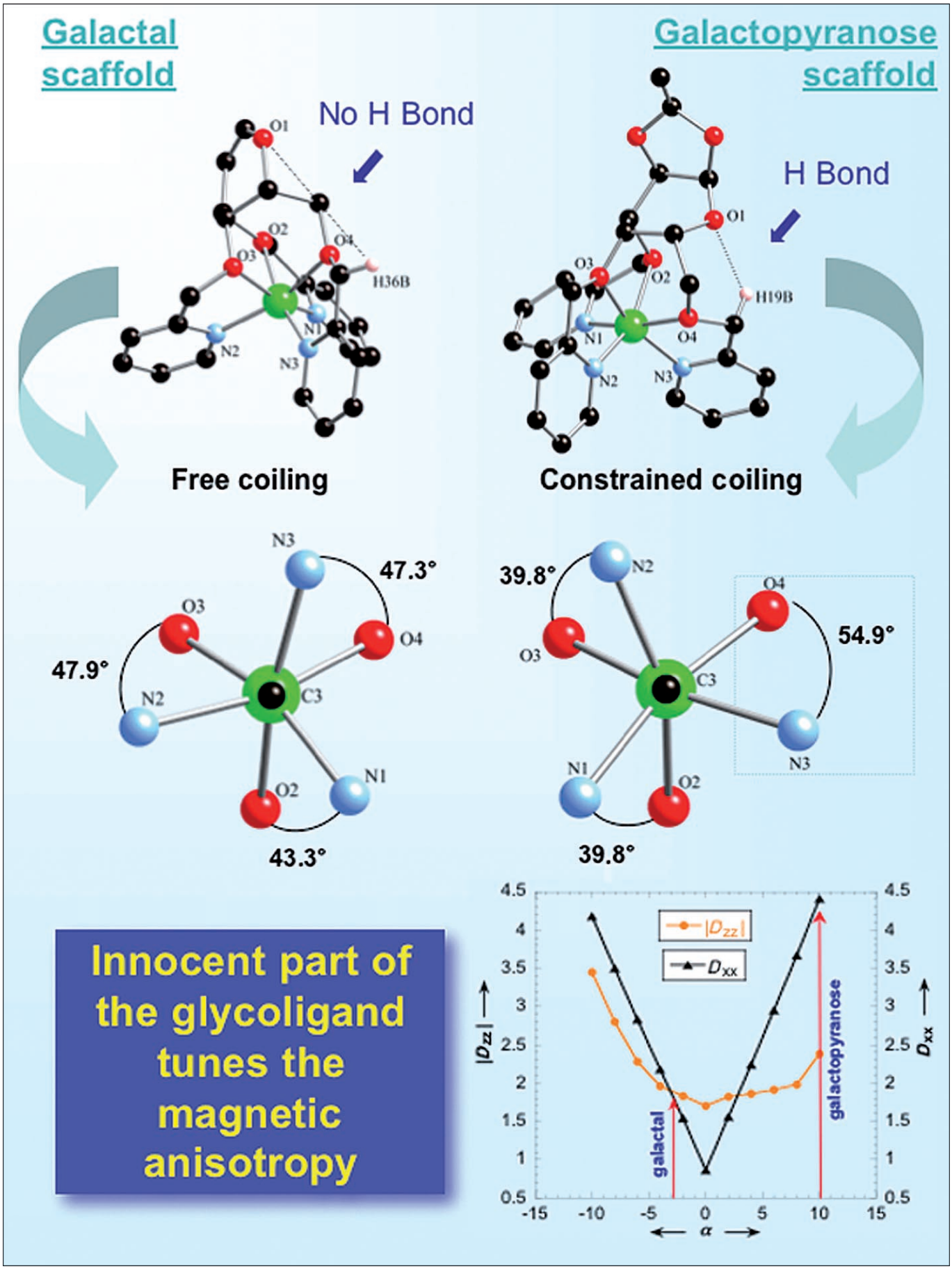

Glycoligands Tuning the Magnetic Anisotropy of Ni^{II} Complexes

Gaëlle Charron,[b] François Bellot,[a] Federico Cisnetti,[a] Giorgio Pelosi,[c] Jean-Noël Rebilly,[b] Eric Rivière,[b] Anne-Laure Barra,[d] Talal Mallah,*[b] and Clotilde Policar*[a]

Abstract: Two organic ligands based on a sugar-scaffold derived from galactose and possessing three O-CH_2-pyridine pendant arms at the 3-, 4-, and 5-positions of the galactopyranose that act as chelates afford mononuclear complexes when reacted with a Ni^{II} salt. The magnetization behavior in the form of $M = f(H/T)$ plots suggests the presence of appreciable magnetic anisotropy within the two complexes. The analysis of the EPR spectra performed at two different temperatures (7 and 17 K) and at three frequencies (190, 285, and 380 GHz) leads to the conclusion that the anisotropy has a high degree of axiality ($E/D = 0.17$ for the two complexes), but with a different sign of the D parameter. The spin hamiltonian parameters D and E were reproduced for the two complexes by using calculations based on the angular overlap model (AOM). The structural difference between the two complexes responsible of the sign of the D parameters was also determined using AOM calculations. A thorough analysis of the structures showed that the structural differences in the coordination sphere of the two complexes responsible of the different D parameter sign result from the nature of the sugar scaffolds. In complex **1**, the sugar scaffold imposes an intramolecular hydrogen bond with one of the atoms linked to Ni^{II}; this arrangement leads to a distorted coordination sphere and positive D value, while the absence of such a hydrogen bond in complex **2** leads to a less distorted environment around the Ni center and to a negative D value.

Keywords: galactose · magnetic properties · nickel · sugar scaffold

Introduction

Magnetic anisotropy is a crucial parameter responsible for the occurrence of single-molecule magnet (SMM) behavior in magnetic clusters.[1] One of the challenges for chemists in the field of molecular magnetism is to be able to tune and ultimately control the magnetic anisotropy in magnetic molecular clusters, particularly those prepared in a stepwise approach. To do so, the first step consists of imposing anisotropy in simple mononuclear complexes that serve as building blocks for magnetic clusters. For hexacoordinate mononuclear complexes that possess an orbitally nondegenerate spectroscopic ground state, the degeneracy of the spin state is lifted (zero-field splitting or magnetic anisotropy) by second-order spin-orbit coupling only when the symmetry is lower than O_h.[2] The magnitude and the nature of the magnetic anisotropy is directly related to the symmetry of the complex at hand.[3] Mn^{III} complexes with a d^4 electronic structure are the archetypes of such octahedral complexes; they possess a relatively large magnetic anisotropy (axial anisotropy parameter D of around $-5\ cm^{-1}$) as the result of the tetragonal distortion induced by the Jahn–Teller effect.[4] Octahedral Ni^{II} d^8 complexes have an isotropic electronic

[a] Dr. F. Bellot, F. Cisnetti, Dr. C. Policar
ICMMO UMR CNRS 8182
Equipe Chimie Bioorganique et Bioinorganique
Univ Paris Sud, 91405, Orsay (France)
Fax: (+33) 1-6915-7231
E-mail: cpolicar@icmo.u-psud.fr

[b] G. Charron, Dr. J.-N. Rebilly, Dr. E. Rivière, Prof. T. Mallah
ICMMO UMR CNRS 8182
Equipe Chimie Inorganique
Univ Paris Sud, 91405, Orsay (France)
Fax: (+33) 1-6915-4754
E-mail: mallah@icmo.u-psud.fr

[c] Prof. G. Pelosi
Dipartimento di Chimica Generale ed Inorganica
Chimica Analitica, Chimica Fisica, Parco Area delle Scienze 17 A
Università di Parma, 43100 Parma (Italy)

[d] Dr. A.-L. Barra
Laboratoire des Champs Magnétiques Intenses
UPR CNRS 5021, 25, avenue des Martyrs, B.P. 166,
38042 Grenoble Cedex 9 (France)

Supporting information for this article is available on the WWW under http://www.chemeurj.org/ or from the author.

distribution in the $d_{x^2-y^2}$ and d_{z^2} orbitals that generally leads to little distortion from the ideal octahedron and thus to weak magnetic anisotropy. The organic ligand may play, for such a case, an important role to bring distortion and thus tune the magnetic anisotropy.[5] Some of us have recently reported a new type of organic ligand in which a polydentate chelating cavity is built onto a sugar ring scaffold; we have named such ligands glycoligands.[6] In this paper, we show that the glycoligands impose a distorted geometry around the Ni^{II} ions. Interestingly, the nature of the magnetic anisotropy is shown to be the result of the nature of the sugar-scaffold supporting the polydentate cavity.

Results and Discussion

Synthesis and crystal structures: Glycoscaffolds derived from galactose have been chosen because the substituents in the 3-, 4-, and 5-positions of the pyranose ring are *cis* and provide a three-fingers claw favorable to chelation.

The synthesis of the two organic ligands **L1** (3,4,6-tri-*O*-(2-picolyl)-1,2-*O*-ethylidene-α-D-galactopyranose) and **L2**

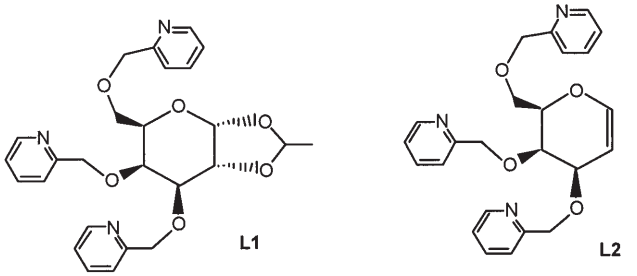

(3,4,6-tri-*O*-(2-picolyl)-D-galactal) can be found elsewhere.[6] The Ni^{II} compounds $[Ni(\mathbf{L1})][PF_6]_2$ (**1**) and $[Ni(\mathbf{L2})][PF_6]_2$ (**2**)were obtained as described below (see Experimental Section).

For **1** and **2**, the molecular structures show that the coordination sphere of the Ni^{II} center is a distorted octahedron with three N_{pyr} and three O_{ether} atoms (Figure 1).[7] The Ni–N and Ni–O bond lengths are mainly the same for the two complexes and range from 2.005 to 2.092 Å. Only one Ni–O distance for each complex is larger than the others (Ni–O2=2.180(6) and Ni–O4=2.117(4) Å for **1** and **2**, respectively). The first coordination sphere around the Ni atoms has pseudo-C_3 symmetry. The octahedra can be described as two coaxial cones, one cone involving the three O_{ether} atoms and the other the three N_{pyr} atoms. The N-Ni-N angles range from 97 and up to 109.6°, while the O-Ni-O angles are all lower than 90°. The average C_3-axis Ni–N angle (noted θ in the following) is close to 64°, while the average C_3-axis Ni–O angles (noted θ') is around 50° leading to a closed NiO_3 and to an open NiN_3 cone apertures for the two complexes. Such angles are all equal to 54.73° for a regular octahedron. The azimuthal angles O–C_3-axis–N (noted φ in the following) involving the N and O atoms belonging to the same pending arm are different in the two complexes: 39.8°, 39.8°, 54.9° for **1** and 47.9°, 47.3°, 43.3° for **2** (Figure 2).[8] The azimuthal angle distribution is signifi-

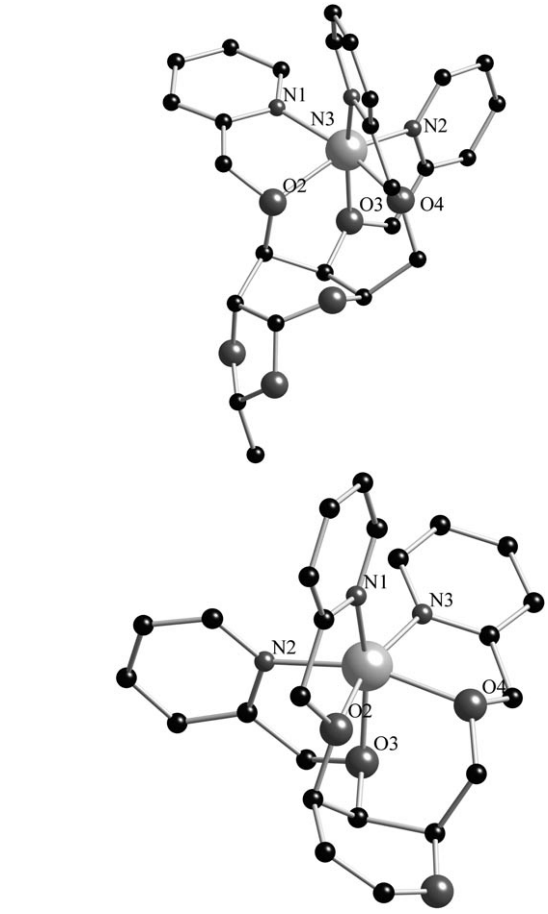

Figure 1. View of the molecular structure of **1** (top) and **2** (bottom).

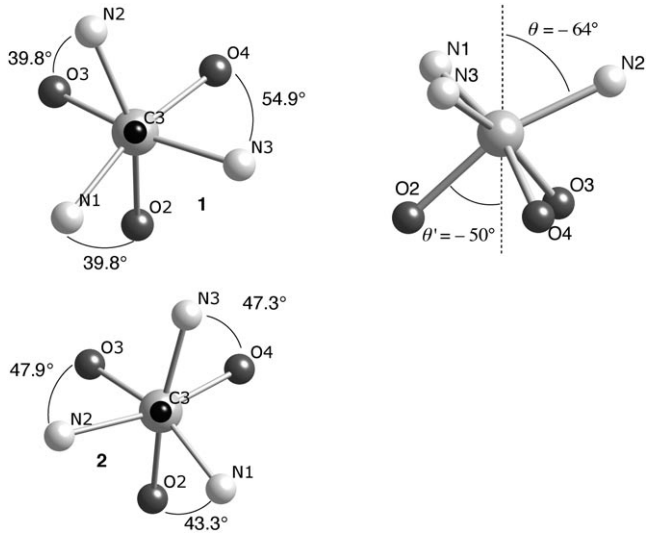

Figure 2. view of the coordination spheres highlighting the Φ values for complexes **1** and **2** (left) and the average values NiO_3 and NiN_3 cone apertures for the two complexes (right).

cantly larger for **1**; this distribution indicates a more distorted Ni environment in **1** than in **2**.

Magnetization studies: The magnetization versus field measurements were performed on crushed crystals sintered in the form of a pellet for both **1** and **2** at $T=2$, 4, and 6 K between 0 and 5.5 T. For both complexes, the magnetization does not saturate at $T=2$ K; it reaches a value slightly lower than 2 μ_B at $\mu_0 H=5.5$ T. The $M=f(\mu_0 H/T)$ plots at different temperatures are not superimposable (Figure 3),

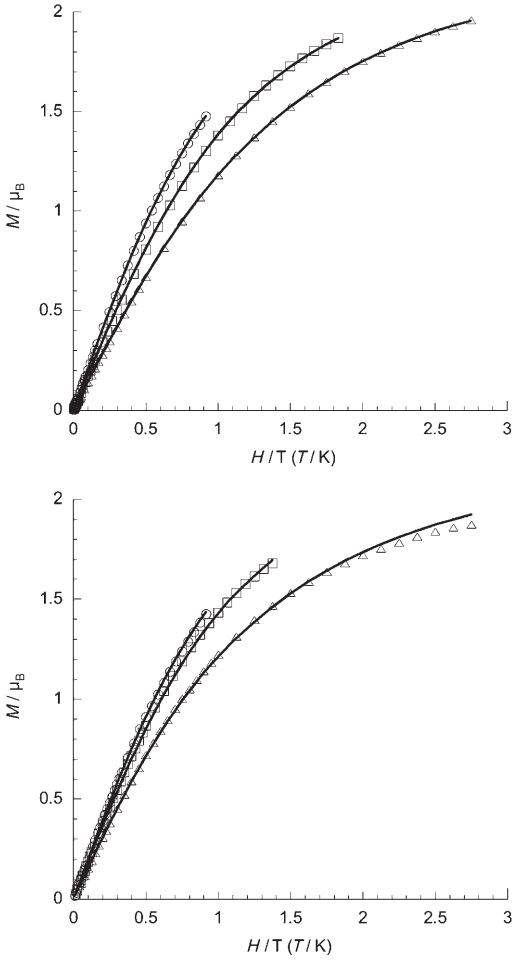

Figure 3. $M=f(H/T)$, at $T=2$ K (△), 4 K (□), 6 K (○) for **1** (top) and **2** (bottom).

indicating the presence of appreciable magnetic anisotropy within the two complexes. The magnetization data were fitted by full diagonalization of the energy matrices for 120 orientations of each value of the magnetic field using a homemade software based on the following spin Hamiltonian: $\boldsymbol{H}=\mu_B \boldsymbol{S}\cdot\boldsymbol{g}\cdot\boldsymbol{B} + \boldsymbol{D}[\boldsymbol{S}_z^2 - S(S+1)/3] + \boldsymbol{E}(\boldsymbol{S}_x^2 - \boldsymbol{S}_y^2)$, in which the first term is the Zeeman effect, and the second and the third terms express the axial and the rhombic anisotropy, respectively. The fit procedure was repeated several times starting from different values. Reasonable fits can be obtained with slightly different $\boldsymbol{E}$ and $\boldsymbol{D}$ values, but without any effect on the sign of the $\boldsymbol{D}$ parameter. The best fits led to the following values for the spin hamiltonian parameters: $\boldsymbol{D}_1=+3.90\ cm^{-1}$, $g_1=2.19$, $\boldsymbol{E}_1=+0.70\ cm^{-1}$, $\boldsymbol{D}_2=-4.60\ cm^{-1}$, $g_2=2.15$ and $\boldsymbol{E}_2=-0.05\ cm^{-1}$ with agreement factors lower than 10^{-5}.

HF-HFEPR studies: To get accurate experimental values for the anisotropy parameters, HF-HFEPR experiments were performed at $T=7$ and 17 K for different frequencies (190, 285, and 380 GHz). The spectra are typical of an $S=1$ spin state. They are dominated by the off-axis turning-point-allowed transition (beta transition) appearing at low field.[3] The spectra of **1** at 285 GHz (Figure 4, top) showed (apart from the beta transition at 3.97 T) four other bands at $\mu_0 H=4.63$, 5.87, 7.93, and 9.87 T (the band at 5.7 T is due to the higher harmonic frequency 380 GHz (Figure S1 in the Supporting Information). To assign the transitions observed in the experimental spectra, the variation of the Zeeman energy levels as a function of the field were calculated for

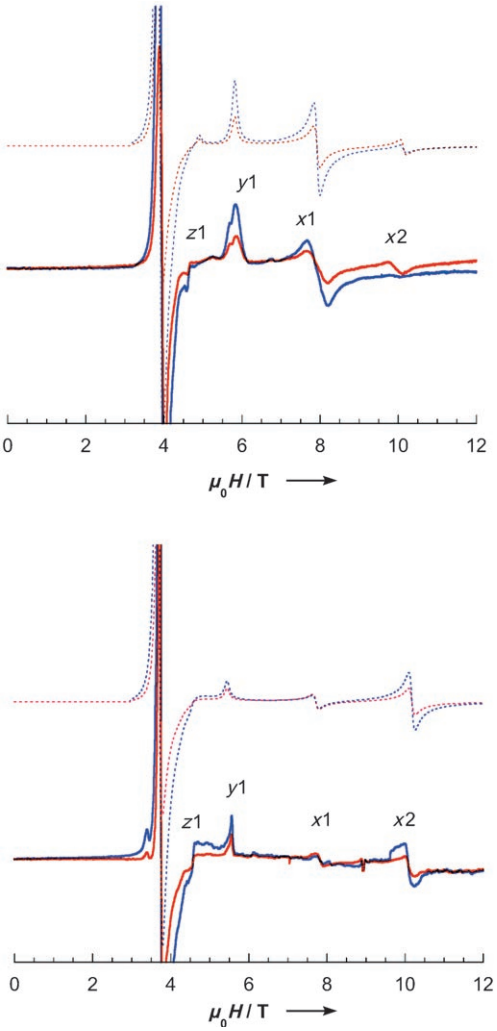

Figure 4. HF-HFEPR spectra at $T=7$ K (blue) and 17 K (red) and $\nu=285$ GHz for **1** (top) and **2** (bottom), experimental (——) and best fit (-----).

the x, y, and z directions of the applied field by using the $\boldsymbol{D}$ and $\boldsymbol{E}$ values obtained from the magnetization data (Figure S2 in the Supporting Information). The expected transitions for each direction for a frequency $\nu = 285$ GHz are indicated on the $\boldsymbol{E} = f(\mu_0 H)$ diagrams; the beta transition is expected to be around the same field value (≈ 4 T) for all directions, which is at the origin of the rather high intensity of the associated band. According to Wassermann nomenclature,[9] the first band peak in the 285 GHz spectra (at 4.63 T) can be assigned to the first z transition ($z1$), while the three following bands were assigned to $y1$, $x1$ and $x2$. The $y2$ and the $z2$ transitions were out of range for the available magnetic field. On the other hand, the $\boldsymbol{E} = f(\mu_0 H)$ plots clearly showed that the intensities of the $y1$ and $x1$ transitions increase upon cooling, while that of the $x2$ transition had the opposite behavior when $\boldsymbol{D}$ is positive. These are actually the observed characteristics of the experimental spectra at $\nu = 285$ GHz (Figure 4 top) that confirm the positive sign of $\boldsymbol{D}$ for **1**. For an $S = 1$ spin system with rhombic anisotropy, the two z transitions are separated by $2\boldsymbol{D}_1/g_z\mu_B$. Assuming, for simplicity as a first approximation, that the centers of the x and z transitions were superimposed ($g_x = g_z$), $\boldsymbol{D}_1/g_z\mu_B$ given by $(H_{x2} + H_{x1})/2 - H_{z1}$ leads to $\boldsymbol{D}_1 = +4.60$ cm^{-1}. Having these hypotheses in mind, it was possible to simulate the EPR spectra of complex **1**.[10] The best simulation for the three spectra [380 GHz (Figure S1), 285 GHz (Figure 4, top) and 190 GHz (Figure S3)] led to the following set of parameters: $\boldsymbol{D}_1 = +4.40$ cm^{-1}, $\boldsymbol{E}_1 = 0.75$ cm^{-1}, $g_{x1} = 2.17$, $g_{y1} = 2.17$ and $g_{z1} = 2.20$. For complex **2**, the analysis of the EPR spectra (at 190, 285 GHz and $T = 7$, 17 K) were carried out in a way similar to **1**. The intensities of the transitions showed the opposite behavior to complex **1** leading to a negative $\boldsymbol{D}$ value (Figure S4, $\nu = 190$ GHz and Figure 4 bottom, $\nu = 285$ GHz). The best fit of the spectra led to the following values: $\boldsymbol{D}_2 = -4.83$ cm^{-1}, $\boldsymbol{E}_2 = -0.82$ cm^{-1}, $g_{x2} = 2.17$, $g_{y2} = 2.16$, and $g_{z2} = 2.20$. The complexes have the same degree of axiality, since their $\boldsymbol{E}/\boldsymbol{D}$ values are equal to 0.17. However, the nature of the magnetic anisotropy is different; for **2** there is an easy axis of magnetization ($\boldsymbol{D} < 0$), while for **1** the magnetization lies mainly in a plane ($\boldsymbol{D} > 0$).

Angular overlap calculations: To analyze the relationship between the structure of the two complexes and the nature of their magnetic anisotropy, we carried out calculations of the anisotropy parameters by using a software based on the angular overlap model (AOM), which enabled us to compute the spin Hamiltonian parameters and to determine the orientation of the $\boldsymbol{D}$-tensor axes based on the structure of the complexes.[11–13] This is a necessary first step for checking whether the experimental data can be reproduced by calculations and to validate the AOM parameters chosen. The calculations for **1** and **2** led to the following values: $\boldsymbol{D}_1 = +6.20$ cm^{-1}, $\boldsymbol{E}_1/\boldsymbol{D}_1 = 0.26$ and $\boldsymbol{D}_2 = -3.80$ cm^{-1}, $\boldsymbol{E}_2/\boldsymbol{D}_2 = 0.14$. These calculated values reproduced reasonably well the magnitude and more importantly the sign of the experimental $\boldsymbol{D}$ parameters. To check that the values of the AOM parameters taken from literature are valid, several calculations were carried out by slightly changing these parameters around the values used. The sign of the as calculated $\boldsymbol{D}$ values have been found to be stable for each complex; only a large (unphysical) change of these parameters allows to severely affect the sign of $\boldsymbol{D}$.

Other important information that can be obtained from the computation is the orientation of the $\boldsymbol{D}$-tensor axes. For complex **2**, the orientation of the principal $\boldsymbol{D}$-tensor axis was found to be relatively close to the pseudo-threefold axis defined above, as expected for a complex of C_3 symmetry for a negative $\boldsymbol{D}$ value (the anisotropy axis displayed an angle of 24.5° with the pseudo-C_3 symmetry axis, Figure 5

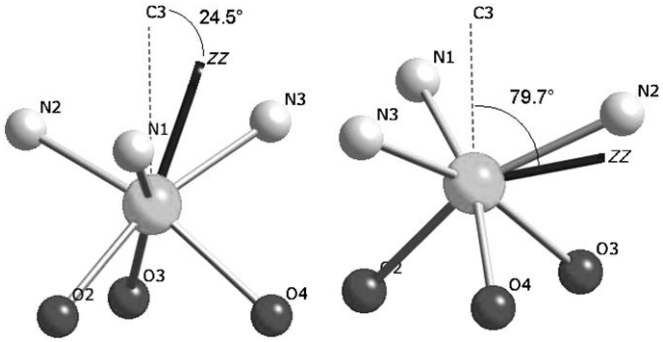

Figure 5. orientation of the principal $\boldsymbol{D}$ tensor axis for **2** (left) and **1** (right).

left). For the more distorted complex **1**, the principal $\boldsymbol{D}$-tensor axis was found to lie perpendicular to the pseudo-threefold axis (it displayed an angle of 79.7° with the pseudo-C_3 symmetry axis, Figure 5 right). Even though it was possible to reasonably reproduce the magnitude of the spin Hamiltonian parameters and to obtain the right experimental sign for $\boldsymbol{D}$, the origin of the difference in the sign of $\boldsymbol{D}$ between the two complexes remains obscure at this stage. To get a clear insight of the structural effects that govern the magnitude and the difference in the sign of the spin Hamiltonian parameters, we undertook systematic calculations of these parameters by considering different model complexes. A highly symmetrical coordination sphere was first considered and then the symmetry was lowered step-by-step to reach one very close to that of the real complexes. The first model complex chosen has D_{3d} symmetry, with six identical ligands and an azimuthal angle $\varphi = 60°$. The other two parameters of the D_{3d} symmetry that define the NiN_3 (or NiO_3) cone aperture (θ) and the M–ligand bond lengths (e_σ) were taken as the corresponding average values of the nitrogen atoms in the real complexes : $\theta = 64°$ (and thus $\theta' = 64°$) and $e_\sigma = 5000$ cm^{-1}. For such a highly symmetrical model complex (MC1), the computed $\boldsymbol{D}$ value was found equal to -1.1 cm^{-1} and the anisotropy axis lying colinear to the threefold symmetry axis as expected. For the second model complex, we performed a "geometrical" symmetry lowering of MC1 by decreasing the NiO_3 cone aperture from $\theta' = 64°$ to $\theta' = 50°$ (which corresponds to the aver-

age angle values of the NiO_3 cone in the real complexes, see above) keeping everything else equal (MC2); a ***D*** value of $-0.8\,cm^{-1}$ was computed. This result shows that lowering the symmetry from D_{3d} to C_{3v} by just closing the NiO_3 cone aperture has little effect on the magnitude of the anisotropy of the complex and does not lead to a change of sign for ***D***. Another possible way to lower the symmetry from D_{3d} to C_{3v} is to differentiate N and O donors ("electronic symmetry lowering"). This can be done by using the AOM parameter e_σ of the oxygen atoms for one of the cones: replacing 5000 by $2700\,cm^{-1}$, which corresponds to the average e_σ value of the oxygen atoms in the real complexes (MC3), and keeping everything else equal to MC1. The computed ***D*** value was found equal to -2.7 in this case instead of $-1.1\,cm^{-1}$ for the more symmetrical complex. This increase in the magnitude of ***D*** is not surprising, since it is known that, all else being equal, the weakening of the ligand field strength reduces the energy separation in the ground-excited terms and thus increases the magnitude of ***D***. The third step consisted in performing both a "geometrical" and an "electronic" symmetry lowering ($\theta=64°$, $\theta'=50°$, $e_\sigma(N)=5000\,cm^{-1}$ and $e_\sigma(O)=2700\,cm^{-1}$: MC4): the ***D*** value obtained ($-2.1\,cm^{-1}$) shows clearly that 1) the two effects are not complementary and 2) the "electronic" effect is the dominant one responsible for the increased negative value of ***D***. The structure of the model complex MC4 is close to that of the complexes **1** and **2**, the only main difference concerns the azimuthal angle (φ), which is equal to 60° in the model complex MC4. For complexes **1** and **2**, φ is far from 60° and more importantly it has different values in each complex. To take into account the structural effect of this angle on the sign of ***D***, we proceeded in two steps. The first step consisted of performing the calculations with a value of φ_{av} taken as the average value of the six azimuthal angles of the two complexes ($\varphi_{av}=45.5°$), and then calculating the ***D*** values with the exact angles found for complexes **1** and **2**. This allows us to check two different structural effects on ***D***: 1) the deviation of φ from 60° to the average value (45.5°) and 2) the magnitude of the distribution of the three φ angles in each complex, since this distribution is larger for **1** than for **2**. The ***D*** value computed for the model complex with $\varphi_{av}=45.5°$ (MC5) was found equal to -2.6 instead of $-2.1\,cm^{-1}$. The deviation from the geometry with $\varphi_{av}=60°$ to that with $\varphi_{av}=45.5°$ led to an increase in the magnitude of ***D***, but has no effect on its sign. The second structural effect to be checked is the distribution of the values of the φ angles in the two complexes. A calculation was thus carried out on a model complex (MC6) with the same three φ angles as for complex **2** (47.9, 47.3 and 43.3°). A ***D*** value of $-2.7\,cm^{-1}$ was obtained. The first conclusion that can be drawn at this level is that for complexes with a threefold symmetry axis the major effect that leads to a large ***D*** value stems from the presence of two different types of ligands inducing different electronic effects on the metal ion. The symmetry lowering from C_{3v} ($\varphi=60°$) towards C_3 ($\varphi=45.5°$) increases the magnitude of the uniaxial magnetic anisotropy and does not allow a change in its nature. And finally, if the three azimuthal φ angles are slightly different (weak distribution), a larger negative ***D*** value is obtained.

As shown in Figure 2, the distribution in φ angles for complex **1** is larger than for **2**. A calculation was thus carried out for a model complex with φ equal to those found for complex **1** (39.8, 39.8 and 54.9°: MC7) and ***D*** was found equal to $+6.6\,cm^{-1}$. Thus, the crucial structural parameter responsible of the difference in the sign of ***D*** between complexes **1** and **2** is the extent of the distribution of the φ angles. Everything else being equal, a large φ distribution leads to a positive ***D*** value, while a weak distribution keeps the ***D***-value negative.

Since the origin of the ***D***-value sign seems to be related to the azimuthal angle distribution, it is important to check how the sign change occurs when the φ angles distribution evolves from 0 to a value as close as possible to that of complex **1** (20.1°).[14] To do so, a model complex MC5α with the three azimuthal angles equal to $45.5+\alpha$, $45.5-\alpha/2$, and $45.5-\alpha/2$ were considered and the ***D*** values were computed for α between -10 and 10°, which corresponds to a maximum distribution of the azimuthal angles of 20° and a minimum of 0.[15] The results are plotted (Figure 6) as $|D_{zz}|$ and

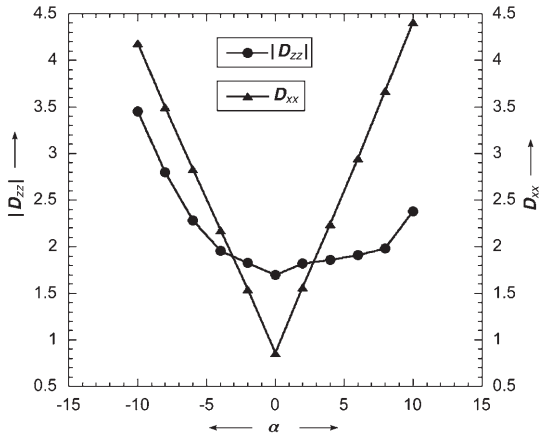

Figure 6. Computed values of the $|D_{zz}|$ and D_{xx} matrix elements of the ***D*** tensor as a function of the angle α that expresses the deviation of the azimuthal angle φ from the average value for the model complex. The D_{zz} and the D_{xx} parameters are matrix elements of the ***D*** tensor. We assumed, for simplicity, that the z axis is the one closest to the pseudo-threefold symmetry axis for all α values even when the D_{xx} value becomes larger than the absolute value of D_{zz}.

D_{xx} as a function of α.[16] The striking feature in Figure 6 is that the ***D*** value is negative ($|D_{zz}|>D_{xx}$) only for a short range of α (between -3 and $+3°$, which corresponds to a φ distribution of 6°, and becomes positive ($D_{xx}>|D_{zz}|$) for all other values of α. The calculated distributions correspond to α values around 10 and $-2.9°$ for complexes **1** and **2**, respectively. Thus, very small differences between the φ angles or, in other words, a slight deviation from the canonic C_3 symmetry, has a dramatic effect on the nature of the magnetic anisotropy. Complex **2** that possesses a weak φ distribution (5.7° for $\alpha=-2.9°$) still has a negative ***D*** value (uniaxial anisotropy), while the large φ distribution (20.1° for $\alpha=10°$)

found for **1** leads to a positive ***D*** value (the largest matrix element is positive) and thus to a planar magnetic anisotropy.

Up to now, all the calculations were performed on model complexes in which the small structural changes between the two complexes have been averaged and only the effects presented above were considered with ideal symmetries. To confirm that the sign of the ***D*** values is indeed directly related to the magnitude of the distribution of the azimuthal angles (as found from the analysis carried out above) and not from other structural differences that were not considered in model complexes, we performed two other calculations on two *chimera* complexes: $\mathbf{1}^{\mathbf{2}}$ and $\mathbf{2}^{\mathbf{1}}$. The chimera complex $\mathbf{1}^{\mathbf{2}}$ has the same structure (bond lengths and angles) as complex **1** apart from the azimuthal angles φ that were set equal to those of complex **2**, while $\mathbf{2}^{\mathbf{1}}$ has all the structural features of **2** but with the azimuthal angles of **1**. The calculated magnetic anisotropy parameters for $\mathbf{1}^{\mathbf{2}}$ were found to be almost the same as those for **2** ($\boldsymbol{D} = -3.3\ \mathrm{cm}^{-1}$ and $\boldsymbol{E}/\boldsymbol{D} = 0.22$) with an angle between the principal ***D***-tensor axis and the C_3 axis equal to 19.5° (to be compared to 24.5° in **2**, Figure S5). The same result was found for complex $\mathbf{2}^{\mathbf{1}}$ ($\boldsymbol{D} = +6.2\ \mathrm{cm}^{-1}$, $\boldsymbol{E}/\boldsymbol{D} = 0.27$), with the principal ***D***-tensor axis lying as for **1** (Figure S6). These results confirm the conclusion of the above calculations that the structural parameter responsible for both the sign of the ***D*** parameters and the orientation of principal ***D***-tensor axes is indeed the larger distribution in the φ azimuthal angles for **1** than for **2**.

Influence of the organic ligand: The structural analyses for **1** and **2** do not reveal any intermolecular interactions responsible for the difference in the distribution of the azimuthal angles. However, for **1** an intramolecular hydrogen bond involving the H19B proton bound to the carbon atom C19 and the oxygen atom O1 of the glycoscaffold is present, while no such interaction can be found for the less distorted complex **2** (Figure 7).[17] Actually for **1**, the ethylidene moiety is a conformational lock imposing a boat conformation ^{O1,C3}B for the glycoscaffold,[18,19] with a dihedral angle O3-C4-C5-C6 of 7.1°. This angle induces a boat conformation for the Ni cycle (Figure 8). The resulting spatial atomic disposition is compatible with a hydrogen bond between H19B and O1, with a distance d(H19B,O1) of 2.37 Å.[17] This hydrogen bond moves C19 towards the sugar cycle and imposes an O4–C_3-axis–N3 azimuthal angle clearly larger than the other two. In **2**, the 1,2-galactal scaffold shows a twist $^{C5}T_{C4}$ conformation, with a dihedral angle O3-C4-C5-C6 of 64.4°. This angle leads to an unconstraint conformation for the Ni cycle, thus leading to the expected more stable chair conformation.[20] Moreover, the twist conformation of the sugar precludes any hydrogen bond involving O1 and a methylene moiety from any of the pending arms ($d > 4$ Å). These structural features lead to a different coiling up of the pending arms and thus to a weak azimuthal angles distribution in complex **2**.

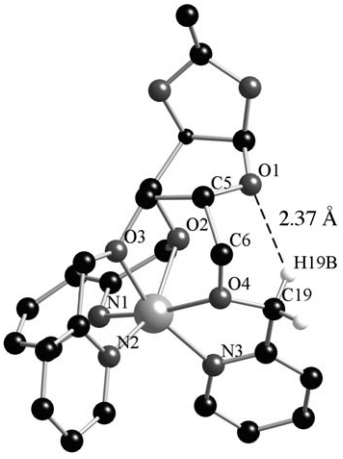

Figure 7. view of **1** highlighting the intramolecular hydrogen bond.

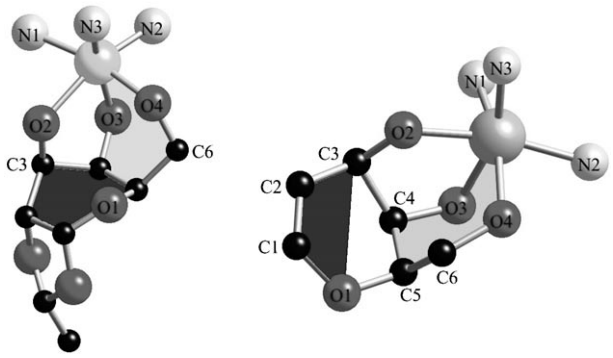

Figure 8. view of the structures including the sugar scaffolds for **1** (left) and **2** (right).

Conclusion

Complexes **1** and **2** were made from two very similar organic ligands derived from galactose and possessing the same three pendent arms that chelate the Ni^{II} ions. An analysis of the ***D*** values of model complexes revealed that the important structural parameter that governs the magnetic anisotropy is the distribution of the three azimuthal angles (φ) involving the O and N atoms of the same pendant arm of the chelating ligand. A weak distribution of this angle (small difference between the three azimuthal angles) has little effect on the nature of the anisotropy when compared to the canonic complex with C_3 symmetry, while a large distribution changes the anisotropy axis from being colinear to the threefold axis to almost perpendicular leading to a positive ***D*** value (easy plane of magnetization) instead of a negative ***D*** value (easy axis). We have shown that the larger distribution of the azimuthal angles is directly linked to the sugar scaffold and not to the bidentate O–N arms that chelate the metal ions. Indeed, an intramolecular hydrogen bond between the sugar scaffold and one O atom of the coordination sphere of the metal ion is at the origin of this larger distortion observed in complex **1**. To the best of our knowl-

edge, this is one of the few systems for which it has been shown how the "innocent" part of the organic ligand determines the nature of the Ni^{II} magnetic anisotropy.

Experimental Section

Synthesis: Synthesis of $[Ni(\mathbf{L1})][PF_6]_2$ (**1**) and $[Ni(\mathbf{L2})][PF_6]_2$ (**2**). The typical protocol for compounds **1** and **2** is described here in detail for the case of compound **1**. Ligand **L1** (107 mg, 0.22 mmol) was dissolved in absolute EtOH (3 mL). A solution of $Ni(NO_3)_2{\cdot}6H_2O$ (70 mg, 0.24 mmol) in absolution EtOH (3 mL) was added dropwise. The color changed from green to azure and a precipitate was obtained that was redissolved by addition of a minimum of acetone. NH_4PF_6 (145 mg, 0.89 mmol) in absolute EtOH (2 mL) was added. Crystals suitable for diffraction are obtained the day after.

*Data for [Ni(**L1**)][PF$_6$]$_2$ (**1**)*: Yield 74%; elemental analysis calcd (%) for $C_{26}H_{29}NiN_3O_6{\cdot}P_2F_{12}$: C 37.71, H 3.53, N 5.07, P 7.48, F 27.53, Ni 7.09; found: C 37.67, H 3.48, N 5.12, P 7.52, F 27.59, Ni 7.03; MS-ES (+): *m*/*z* (%): 268.7 (100) $[M]^{2+}$, 480.1 (22) $[M-Ni+H]^+$, 502.3 (91) $[M-Ni+Na]^+$, 572.2 (17.4) $[M+Cl]^+$.*Data for [Ni(**L2**)][PF$_6$]$_2$ (**2**)*: Yield 65%; elemental analysis calcd (%) for $C_{24}H_{25}NiN_3O_4{\cdot}P_2F_{12}$: C 37.55, H 3.28, N 5.48, P 7.55, F 29.72, Ni 7.55; found: C 37.42, H 3.11, N 5.33, P 7.02, F 26.23, Ni 7.27; MS-ES (+): *m*/*z* (%): 238.7 (71) $[M]^{2+}$, 442.3 (100) $[M-Ni+Na]^+$, 515.2 (2.5%) $[M+Cl]^+$.

Crystallographic analyses: The structures were refined by using SHELXL97.[21] The refinement procedure was carried out using the WinGX package[22] with the program PARST.[23]

*Crystal data for **1***: $C_{26}H_{29}NiN_3O_6{\cdot}P_2F_{12}$, $M_r=828.17$, azure prisms, crystal size $0.20\times0.35\times0.42$ mm^3, orthorhombic, space group $P2_12_12$, $a=16.750(4)$, $b=18.897(5)$, $c=10.124(3)$ Å, $V=3204(1)$ Å^3, $T=298$ K, $Z=4$, $\rho_{calcd}=1.716$ g cm^{-3}, $\mu(Mo_{K\alpha})=8.21$ cm^{-1}, $F(000)=1680$; a total of 5196 reflections up to $h(0/23)$, $k(0,26)$, $l(0/14)$ in the range $3<\theta<30$, of which 5167 were unique and 4124 observed with $F_o>4\sigma(F_o)$, 452 parameters, $R1_{obs}=0.069$, $wR2_{obs}=0.178$, GOF = 0.848, Flack parameter −0.07(4), max/min residual electron density 0.47/−0.47 e Å^{-3}.

*Crystal data for **2***: $C_{24}H_{25}NiN_3O_4{\cdot}P_2F_{12}$, $M_r=768.117$, azure prisms, crystal size $0.212\times0.34\times0.40$ mm^3, monoclinic, space group $P2_1$, $a=9.195(2)$, $b=10.393(2)$, $c=15.358(3)$ Å, $\beta=90.62(1)°$, $V=1467.6$ (5) Å^3, $T=298$ K, $Z=2$, $\rho_{calcd}=1.738$ g cm^{-3}, $\mu(Mo_{K\alpha})=8.84$ cm^{-1}, $F(000)=776$; a total of 14302 reflections up to $h(-10/10)$, $k(-12/12)$, $l(-18/18)$ in the range $3<\theta<25$, of which 5198 were unique ($R_{int}=0.0633$) and 2887 observed with $F_o>4\sigma(F_o)$, 415 parameters, $R1_{obs}=0.049$, $wR2_{obs}=0.122$, $R1_{all}=0.093$, GOF = 0.958, Flack parameter 0.059(22), max/min residual electron density 0.38/−0.38 e Å^{-3}.

CCDC-608840 and CCDC-608841 contain the supplementary crystallographic data for this paper. These data can be obtained free of charge from The Cambridge Crystallographic Data Centre via

www.ccdc.cam.ac.uk/data_request/cif.

Magnetic measurements: Magnetization measurements were performed by using a Quantum Design MPMS5 SQUID magnetometer. HF-HFEPR experiments were performed at the High Magnetic Field Laboratory, Grenoble (France), by using a previously described apparatus.[24] Ground crystals (about 30 mg for EPR and 5 mg for SQUID) pressed to form a pellet in order to reduce torquing effect under high magnetic fields were used. Simulation program is available from Dr. H. Weihe; for more information see the WWW page:

http://sophus.kiku.dk/software/epr/epr.html.[11]

Acknowledgements

The authors thank the CNRS (Center National de la Recherche Scientifique), the European Community (contract MRTN-CT-2003–504880/RTN Network "QuEMolNa" and contract NMP3-CT-2005–515767 NoE "MAGMANET"), and the French Ministry of Science for financial support through the program ACI "Jeunes Chercheurs" 2004. The authors also thank H. Weihe for provision of the SimRPE program and A. Bencini for provision of the AOM program.

[1] a) D. Collison, M. Murrie, V. S. Oganesyan, S. Piligkos, N. R. J. Poolton, G. Rajaraman, G. M. Smith, A. J. Thompson, G. A. Timko, W. Wernsdorfer, R. E. P. Winpenny, E. J. McInnes, *Inorg. Chem.* **2003**, *42*, 5293; b) A.-L. Barra, A. Caneschi, A. Cornia, A. F. Fabrizi de Biani, C. Fabretti, D. Gatteschi, C. Sangregorio, R. Sessoli, L. Sorace, *J. Am. Chem. Soc.* **1999**, *121*, 5302; c) A. L. Barra, L.-C. Brunel, D. Gatteschi, L. Pardi, R. Sessoli, *Acc. Chem. Res.* **1998**, *31*, 460; d) S. Accorsi, A.-L. Barra, A. Caneschi, G. Chastanet, A. Cornia, A. C. Fabretti, D. Gatteschi, C. Mortalo, E. Olivieri, F. Parenti, P. Rosa, R. Sessoli, L. Sorace, W. Wernsdorfer, L. Zobbi, *J. Am. Chem. Soc.* **2006**, *128*, 4742.

[2] O. Kahn, *Molecular Magnetism*, VCH, Weinheim, **1993**.

[3] F. E. Mabbs, D. Collison, in *Electron Paramagnetic Resonance of Transition Metal Compounds*, Elsevier, Amsterdam, **1992**.

[4] a) A.-L. Barra, D. Gatteschi, R. Sessoli, G. Abbati, A. Cornia, A. C. Fabretti, M. G. Uytterhoeven, *Angew. Chem.* **1997**, *109*, 2423; *Angew. Chem. Int. Ed. Engl.* **1997**, *36*, 2329; b) J. Limburg, J. S. Vrettos, R. H. Crabtree, G. W. Brudvig, J. C. de Paula, A. Hassan, A.-L. Barra, C. Duboc-Toia, M.-N. Collomb, *Inorg. Chem.* **2001**, *40*, 1698

[5] a) J. Krzystek, J.-H. Park, M. W. Meisel, M. A. Hitchman, H. Stratemeier, L.-C. Brunel, J. Telser, *Inorg. Chem.* **2002**, *41*, 4478; b) S. Vongtragool, B. Gorshunov, M. Dressel, J. Krzystek, D. M. Eichhorn, J. Telser, *Inorg. Chem.* **2003**, *42*, 1788; c) G. Rogez, J. N. Rebilly, A. L. Barra, L. Sorace, G. Blondin, N. Kirchner, M. Duran, J. van Slageren, S. Parsons, L. Ricard, A. Marvilliers, T. Mallah, *Angew. Chem.* **2005**, *117*, 1910; *Angew. Chem. Int. Ed.* **2005**, *44*, 1876.

[6] F. Bellot, R. Hardré, G. Pelosi, M. Thérisod, C. Policar, *Chem. Commun.* **2005**, 5414.

[7] Distances for **1** [Å] and angles [°]: Ni1−N1 2.044(9), Ni1−N2 2.046(8), Ni1−N3 2.054(8), Ni1−O2 2.180(6), Ni1−O3 2.031(6), Ni1−O4 2.063(7); N1-Ni1-N2 100.8(3), N1-Ni1-N3 96.4(3), N1-Ni1-O2 78.8(3), N1-Ni1-O3 98.5(3), N2-Ni1-N3 109.6(4), N2-Ni1-O3 77.4(3), N2-Ni1-O4 93.8(3), N3-Ni1-O2 95.4(3), N3-Ni1-O4 79.6(3), O2-Ni1-O3 77.8(2), O2-Ni1-O4 87.6(3), O3-Ni1-O4 83.5(3). The sugar moiety is in a boat (^{O1,C3}B) conformation (QT = 0.649(9) Å, $\theta2=97.5(8)°$ and $\phi2=-5.0(9)°$). The stereochemical environment of the nickel(II) ion is OC-6-52-A. Distances for **2** [Å] and angles [°]: Ni1−O2 2.034(5), Ni1−O3 2.092(4), Ni1−O4 2.117(4), Ni1−N1 2.022(6), Ni1−N2 2.060(6), Ni1−N3 2.005(5); O2-Ni1-O3 81.3(2), O2-Ni1-O4 85.3(2), O2-Ni1-N1 78.0(2), O2-Ni1-N2 90.6(2), O2-Ni1-N3 165.3(2), O3-Ni1-O4 79.9(2), O3-Ni1-N1 159.2(2), O3-Ni1-N2 80.2(2), O3-Ni1-N3 95.8(2), O4-Ni1-N1 100.6(2), O4-Ni1-N2 160.0(2), O4-Ni1-N3 80.1(2), N1-Ni1-N2 97.6(2), N1-Ni1-N3 104.8(2), N2-Ni1-N3 103.2(2). The sugar moiety is in a twist $^5T_4$ conformation (QT = 0.466(8) Å, $\theta2=130$ (1)° and $\phi2=76(1)°$). The stereochemical environment of the nickel(II) ion is OC-6-52-C in **2**.

[8] Such an azimuthal angle is equal to 60° for a regular octahedron.

[9] E. Wasserman, L. C. Synder, W. A. Yager, *J. Chem. Phys.* **1964**, *41*, 1763.

[10] J. Glerup, H. Weihe, *Acta Chem. Scand.* **1991**, *45*, 444.

[11] A. Bencini, I. Ciofini, M. G. Uytterhoeven, *Inorg. Chim. Acta* **1998**, *274*, 90.

[12] A. Bencini, C. Benelli, D. Gatteschi, *Coord. Chem. Rev.* **1984**, *60*, 131.

[13] The AOM parameters for the nitrogen pyridine atoms were taken from similar complexes in the literature and, for oxygen atoms, they were adapted from those of water molecules.[12,13] Only the sigma interactions have been considered. Racah parameters for the Ni^{II} ion: $B=860$ cm^{-1}, $C=3350$ cm^{-1}, $z=600$ cm^{-1}. Parameters for **1**: $e_\sigma=4922$, 4910, and 4804 cm^{-1} for N1, N2, and N3, respectively;

$e_\sigma = 2154$, 3077, and 2846 cm^{-1} for O2, O3, and O4, respectively. Parameters for **2**: $e_\sigma = 5196$, 4734, and 5420 cm^{-1} for N1, N2, and N3 respectively; $e_\sigma = 3053$, 2647, 2500 cm^{-1} for O2, O3, and O4, respectively. It it important to mention here that the AOM parameters may be obtained by fitting the electronic spectra of the complexes. However, because of the rather distrorted geometry of the complexes it is difficult to assign one e_σ value for each atom in the coordination sphere of the metal ions. Since the AOM parameters for Ni^{II} complexes are well referenced in the literature, we prefered to rely on these well accepted values and to adapt them when necessary to our case.

[14] The distribution of the φ angles around the average value of 45.5° was computed to be equal to 21.5 and 5.7° for complexes **1** and **2**, respectively.

[15] The parametrization of the three φ angles by $45.5+\alpha$ and so on allows for given α values to lead to values of the φ angles very close to those found experimentally for the two complexes, but of course not the exact distribution. This does not change at all the conclusions drawn from the general behavior of Figure 6.

[16] The $\boldsymbol{D}_{zz}$ and the $\boldsymbol{D}_{xx}$ parameters are matrix elements of the $\boldsymbol{D}$ tensor. We assumed, for simplicity, that the z axis is the one closest to the pseudo-threefold symmetry axis for all α values even when the $\boldsymbol{D}_{xx}$ value becomes larger than the absolute value of $\boldsymbol{D}_{zz}$.

[17] R. J. Desiraju, *Acc. Chem. Res.* **1996**, *29*, 441–449.

[18] a) J. W. Krajewski, P. Gluzinski, Z. Urbanczyk-Lipkowska, A. Zamojski, G. D. Andreetti, G. Bocelli, *Carbohydr. Res.* **1986**, *148*, 1; b) E. Miler-Srenger, *Carbohydr. Res.* **1989**, *195*, 1; c) J. M. Dianez, M. D. Estrada, A. Lopez-Castro, S. Perez-Garrido, *Z. Kristallogr.* **1998**, *213*, 115; d) M. Cudic, B. Kojic-Prodic, B. Milinkovic, J. Horvat, S. Horvat, M. Elofsson, J. Kihlberg, *Carbohydr. Res.* **1996**, *287*, 1; e) C. Vogel, M. Farouk, M. Michalik, H. Reinke, S. Jarosz, *Pol. J. Chem.* **2005**, *79*, 251; f) C. Foces-Foces, F. H. Cano, S. Garcia-Blanco, *Acta Crystallogr. Sect .B* **1976**, *32*, 3029; g) L. M. Engelhardt, B. W. Skelton, R. V. Stick, D. M. G. Tilbrook, A. H. White, *Aust. J. Chem.* **1990**, *43*, 1657.

[19] $^{X,Y}B$ indicates a boat conformation with X and Y atoms being at the bottom of the boat conformation (O1,C3 for **1**), the other atoms defining a plane. $^{X}T_{Y}$ indicates a twist conformation with two adjacent atoms X and Y being above and below, respectively, the plane defined by the remaining atoms. Similarly, $^{X}C_{Y}$ refers to a chair conformation. For further information, see P. M. Collins, R. J. Ferrier, *Monosaccharides*, Wiley, Chichester, **1996**.

[20] P. Comba, M. Maeder, L. Zipper, *Helv. Chim. Acta* **1989**, *72*, 1029–1037.

[21] G. M. Sheldrick, SHELXL 97—A Program for Structure Refinement, University of Göttingen, Göttingen (Germany), **1997**.

[22] L. J. Farrugia, *J. Appl. Crystallogr.* **1999**, *32*, 837–838.

[23] M. Nardelli, *J. Appl. Crystallogr.* **1995**, *28*, 659.

[24] A.-L. Barra, L.-C. Brunel, J. B. Robert, *Chem. Phys. Lett.* **1990**, *165*, 107.

Received: October 31, 2006
Published online: February 13, 2007

